Crack Growth Modeling and Life Prediction of Pipeline Steels Exposed to Near-Neutral pH Environments: Dissolution Crack Growth and Occurrence of Crack Dormancy in Stage I

JIAXI ZHAO, WEIXING CHEN, MENGSHAN YU, KARINA CHEVIL, REG EADIE, GREG VAN BOVEN, RICHARD KANIA, JENNY BEEN, and SEAN KEANE

This investigation was initiated to provide governing equations for crack initiation, crack growth, and service life prediction of pipeline steels in near-neutral pH (NNpH) environments. This investigation has focused on the crack initiation and early-stage crack growth. The investigation considered a wide range of conditions that could lead to crack initiation, crack dormancy, and crack transition from a dormant state to active growth. It is concluded that premature rupture caused by stress cracking at a service life of about 20 to 30 years previously observed during field operation could take place only when the worst conditions responsible for crack initiation and growth have been realized concurrently at the site of rupture. This also explains the reason that over 95 pct of NNpH cracks remain harmless, while about 1 pct of them become a threat to the integrity of pipeline steels.

DOI: 10.1007/s11661-016-3951-3
© The Minerals, Metals & Materials Society and ASM International 2017

I. INTRODUCTION

PIPELINE transportation is important to the world economy. Transporting crude oil and natural gas *via* pipeline is safer, more reliable, and more economical compared to rail cars and tankers. The safety and integrity of pipelines are a matter of paramount importance because of the hazardous nature of the transported substances. Stress corrosion cracking (SCC) and corrosion fatigue represent a substantial cost to pipeline companies. SCC is controlled from an integrity management point of view by in-line inspection and hydrostatic testing for oil and gas pipelines. These techniques provide protection from in-service failures when used as part of pipeline integrity management process.

It has been determined that the two types of external SCC on underground pipelines are high-pH SCC (classical SCC) and NNpH SCC (Low pH SCC).[1] A common feature of both forms of SCC is that they form crack colonies consisting of up to hundreds of longitudinal surface cracks in the body of pipe that link up to form long, shallow flaws. One of the distinguishing characteristics between the two forms of cracking is their propagation path: NNpH SCC is transgranular, while high-pH SCC is intergranular.[2,3]

Cracking failures of structural components are usually divided into three stages. Crack initiation and early-stage crack growth in Stage I, steady state crack growth in Stage II, and rapid growth leading to final failure in Stage III. During Stage III, the mechanical driving force results in rapid crack growth of a sizable crack and failure is imminent. Integrity management measures should be taken prior to reaching Stage III. Stages I and II provide the opportunity for integrity management. During these two stages, inspection of the structures and steps for the control of crack initiation and growth for service life extension can be performed.

The three stages causing SCC failures of pipeline steels are often described by the bathtub model proposed by Parkins,[4] as shown in Figure 1(a). It conceptually describes the relative rate of crack growth. Crack initiation and early-stage crack growth in Stage I were visualized as occurring relatively quickly with the initial crack growth rate being fast but decreasing as the crack propagates. A steady state crack growth rate was reached in Stage II and fast crack growth rate was seen in Stage III.

Although the relative crack growth rate was visualized in the bath tub model, the detailed mechanisms in each stage were not defined. Under the situation of high-pH SCC, the mechanisms governing crack growth have been well characterized by the repeated processes of crack tip passivation and rupture of the passive film for continuous crack growth. Crack tip advance is directly caused by the dissolution of iron at the crack tip.[4]

JIAXI ZHAO, WEIXING CHEN, MENGSHAN YU, and REG EADIE are with the Department of Chemical and Materials Engineering, University of Alberta, Edmonton T6G 2G6, Canada. Contact e-mail: weixing@ualberta.ca, Weixing.Chen@ualberta.ca KARINA CHEVIL and RICHARD KANIA are with TransCanada Pipelines, 450 1st Street SW, Calgary, AB T2P 5H1, Canada. GREG VAN BOVEN is with Spectra Energy Transmission Ltd., Suite 1100 - 1055 West Georgia Street, Vancouver, BC V6E 3P3, Canada. SEAN KEANE is with Enbridge Pipelines Inc., 10201 Jasper Avenue, Edmonton, AB T5J 3N7, Canada. JENNY BEEN is with IRISNDT-Engineering, Calgary, AB T1Y 7L3, Canada.

Manuscript submitted January 27, 2016.
Article published online January 20, 2017

Modeling of crack growth involving slip-dissolution or film-formation-rupture mechanisms, such as the high-pH SCC of pipeline steels, is relatively well studied.[5–7] In general, the average crack velocity could be related to the crack tip strain rate.[5–7] In this model, crack advance is related by Faraday's law to oxidation reactions (dissolution, passivation, and spontaneous corrosion) which happen at the crack tip as the protective film is ruptured by increasing strain of the underlying metal.[5] Rupture occurs with a periodicity which is computed from the fracture strain of the oxide and the strain rate at the crack tip.[5] By using this slip-dissolution/film model, an improved design and lifetime evaluation of environmental cracking in Boiling Water Reactors (BWR) was proposed for engineering application.[6]

For the cracking of pipeline steels in NNpH environments, the crack tip strain rate has been correlated with the growth rate obtained under cyclic loading.[2,8–10] The correlation is generally very poor, with scatters up to several orders of magnitude. Pipeline steels are not passivated in NNpH soil environments. This has been analyzed as the major reason for the large disagreement between the slip-dissolution or film-formation-rupture model and NNpH crack growth behavior of pipeline steels.[10] In addition, the crack growth behavior of NNpH environments differs from the slip-dissolution or film-formation-rupture model because of the following: (1) although it has traditionally been termed "stress corrosion cracking," crack growth has never been observed under a static loading condition except for during the stage of crack initiation. It was determined later that the cracking is driven by corrosion fatigue mechanisms with some uniqueness. (2) The loading frequencies typically vary over a wide range from 10^{-1} to 10^{-6} Hz, which is usually beyond the scope of most fatigue or corrosion fatigue investigations. (3) The rate of corrosion is typically well below 0.1 mm/year at which a premature failure solely by corrosion would occur after much longer times than are actually observed. (4) Hydrogen, a by-product of corrosion, can be generated to a level at which hydrogen

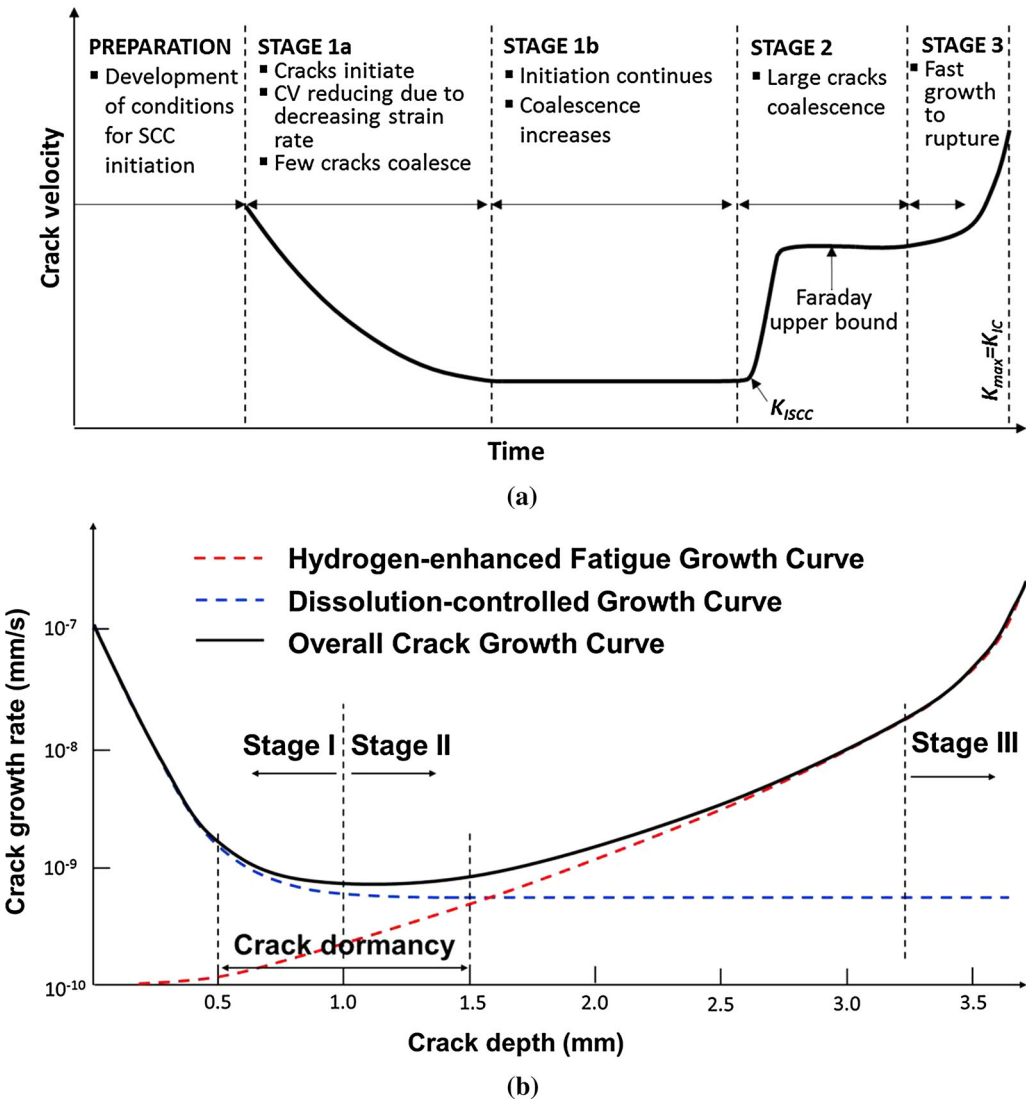

Fig. 1—(*a*) Parkins' SCC model;[4] (*b*) Bathtub model for NNpH stress cracking in present work.[11]

embrittlement may occur only under special conditions. (5) Pipelines are operated under variable pressure fluctuations that may lead to enhanced crack growth resulting from load interaction effects.

This investigation was initiated to address crack growth behavior of pipeline steels in NNpH environments with a full consideration of the uniqueness of the mechanisms involved and the points noted above. The crack advance mechanisms in near-neutral pH environments are very different from the high-pH SCC mechanisms suggested by Parkins. These differences are highlighted in Figure 1(b) using bathtub model.[4,11] Cracking mechanisms in each stage of the bath tub model are also identified. Based on the current understanding of the crack growth mechanisms in NNpH environments, this research is aimed to develop governing equations for crack growth in Stage I and Stage II. This investigation is devoted to the governing equations for crack initiation and early-stage crack growth (Stage I).

II. MECHANISMS OF CRACK INITIATION AND EARLY-STAGE CRACK GROWTH

During early-stage crack growth, the conditions for corrosion have been developed, such as coating damage, ground water in contact with the pipe surface, and ineffective cathodic protection. Crack initiation results from localized corrosion at the pipe surface, leading to crack-like defects. This stage is usually dependent on coating conditions, soil environments, and steel metallurgy. Mechanical driving forces such as operating pressure fluctuations are less important. The rate of dissolution decreases as crack depth increases and many cracks stop growing upon reaching a crack depth of ~1 mm, at which point the crack enters a state of dormancy,[12–14] as shown in Figure 2. The data in Figure 2 are from one pipeline section under NNpH environment, and the depth of most cracks is less than 1.0 mm (see next section for more crack details). Stage I can be controlled or prevented through coating protection and effective cathodic protection.

Initiation can be caused by many different mechanisms[3,13,15–23] including:

1. preferential dissolution at physical and metallurgical discontinuities such as scratches,[15] inclusions,[16] grain boundaries, pearlitic colonies, and banded structures[17–19] in the steel,
2. corrosion along persistent slip bands induced by cyclic loading prior to corrosion exposure,[17,20]
3. crack initiation at stress raisers such as corrosion pits,[21,22] and
4. localized corrosion through various galvanic effects related to mill scale,[23] microstructures,[17,18] and residual stresses.[13]

The initiation of the microstructurally short cracks, usually <100 μm, can occur under constant stress loading. The early crack growth is caused by the presence of high tensile residual stresses at the pipe sub-surface,[3,13,14] which adds to the applied stress. However, these cracks generally go into dormancy for the following reasons:

1. The reduced rate of dissolution at the crack tip in the crack depth direction because of a complicated process involving the gradient of CO_2 and the variation of ionic concentrations in the system: This is believed to be a primary cause for crack dormancy.[10,12–14]
2. The nature and the magnitude of residual stresses at and near the outer surface of pipeline steel:[13,14] Since the residual stress must integrate to zero over cross section, the high tensile residual stresses if present at or close to the outer surface, which is a prerequisite for crack initiation, will usually decrease toward the inner surface, and even become compressive. Thus, as the crack grows it is likely to be under decreasing local stresses at its tip, which may hamper the onset of stage II. In the majority of crack colonies, the overall mechanical driving forces are below the threshold for crack propagation beyond 1 mm and cracks remain in dormancy. In this way the detailed nature and magnitude of residual stresses determine largely when a dormant crack can be reactivated.
3. The level of diffusible hydrogen:[24] Hydrogen acts together with the residual stresses and the chance of remaining at the dormant state will be high if the concentration of diffusible hydrogen in material surrounding the crack tip is low.

Among the above three factors the 1st will be predominant, while the 2nd and 3rd factors contribute little to crack growth in Stage I, but would define the length of dormancy in Stage I. To further understand the importance of the above factors in Stage I, characteristics of cracks from the field will be analyzed in the next section.

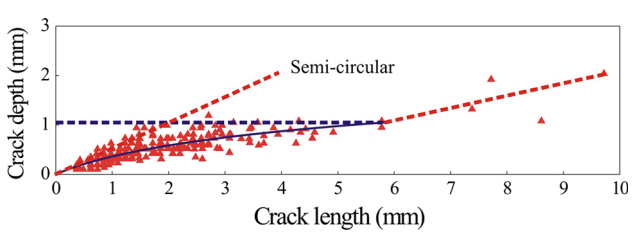

Fig. 2—Field data on correlation of crack depth under NNpH environments.

III. CHARACTERISTICS OF CRACKS FROM THE FIELD

In order to develop the governing equations representative of cracking mechanisms found in the field, a X-65 pipe piece fractured in the field caused by NNpH cracking was analyzed. The pipeline had been in service for 19 years before the rupture. Part of the pipe piece was deformed due to rupture. The pipe piece was sectioned into seven metallurgical samples containing

typical crack colonies. These crack colonies were all from regions with little deformation. The metallurgical samples containing crack colonies were mounted in resin with the pipe surface at the top. Each of the samples was ground and polished down the pipe thickness direction to examine crack morphologies. The grinding steps were generally controlled to about 0.1 mm deep, and were quite a bit smaller for shorter cracks in order to achieve sufficient resolution in the crack depth direction. Images of the cracks at various grinding steps were recorded by a digital camera attached to an optical microscope with a magnification ranging from 50 to 1000 times. The images were analyzed to determine both the crack length and crack depth.

A total of 285 cracks from the undeformed seven colonies were analyzed. Approximately 1 pct of cracks were found to have a crack depth larger than 1.0 mm, as seen in Figure 2, which correlates the crack depth with crack surface length. The dashed line in Figure 2 represents the crack depth/length ratio of 0.5, which indicates a semi-circular shape (Left red dashed line in Figure 2). As shown in Figure 2, the crack ceases to grow or grows slowly in the depth direction while crack depth reaches 1.0 mm, which indicates the crack growth in the depth direction gradually decreases with an increase in crack length. This is a widely observed feature of NNpH SCC cracks, which is often referred to as crack dormancy. In general, less than 5 pct of cracks found in crack colonies were found to be able to grow continuously or discontinuously to a critical size leading to rupture.[25] As a crack grows, the mechanical driving forces (stress intensity factor) become higher, which should lead to an increase in crack growth rate. This is clearly contradicted the observation of crack dormancy in the depth direction as shown in Figure 2.

It would be expected that crack growth would be governed by the principles of fracture mechanics when the stress intensity factor becomes appreciable. Since stress intensity increases with crack depth, fracture mechanics should become important as the crack dimensions increase. According to fracture mechanics, a semi-elliptical crack with its long axis parallel to pipe surface would yield the highest stress intensity factor at the depth tip where a higher growth rate can be expected such that a semi-circular shape, as illustrated in Figures 2 and 3, could be formed. This is inconsistent with the crack profiles found from the field, since the ratio of crack length to depth is much higher than 2.0 (see Figure 2). Therefore, the occurrence of dormancy should not be driven by mechanically related conditions, although such mechanical conditions could extend or shorten the stage of dormancy which is to be discussed later.

The microstructure of pipeline steels within a distance of 1 mm from the surface can be considered homogeneous, although banded microstructure could be found toward the middle wall of pipe. This indicates that the reduced rate of dissolution is not likely caused by any possible metallurgical factors in the depth direction. It has been widely accepted that the decreased rate of corrosion at the crack tip is attributed, on one hand, to the reduced galvanic effect of corrosion[13,23] and the

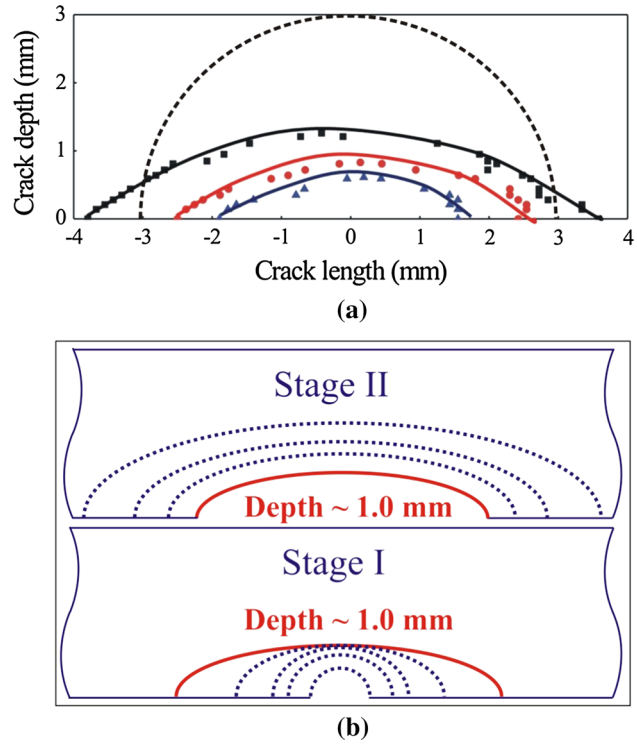

Fig. 3—(*a*) Crack shape evolution under NNpH environments; (*b*) crack advance characteristics in stage I and II.

decreased CO_2 diffusion to the crack tip as the crack becomes deeper.[26]

The cracked oxide scale or mill scale on the pipeline surface is believed to form a galvanic couple with the steel substrate at the bottom of the cracks within the mill scale.[23] The rate of dissolution is inversely related to the pH of the solutions.[10] Lower CO_2 levels in the environments yield higher pH of the solution in general. Much reduced corrosion was also observed at the bottom of a simulated disbonded coating with a narrow disbonding gap as compared with the corrosion at open mouth of the gap where CO_2 level is highest.[26] It has also been observed that a galvanic cell can be formed between the region with low/compressive residual stress and the region with high/tensile residual stresses.[13]

From the above discussion, it is obvious that different mechanisms are operating in Stage I and Stage II. As illustrated in Figures 3(a) and (b)), Stage I growth is primarily driven by the direct dissolution of iron at confined areas to form cracks and at the crack tip during early stage of crack growth, Mechanically driven processes become predominant in Stage II (see Figure 3(b)), which is to be discussed in Reference 27.

IV. GOVERNING EQUATIONS FOR CRACK INITIATION AND EARLY-STAGE GROWTH

Based on the mechanisms of crack initiation and early-stage crack growth as introduced above, mathematic equations governing crack growth can be developed. First, the following three boundary conditions are defined.

A. *Boundary Condition 1*

At the beginning of crack initiation, for a defect-free pipeline, the environment is isotropic in any direction, and therefore the same rate of dissolution occurs both in the depth direction and along the surface. Crack depth, a, and crack length, $2c$, at the beginning of crack initiation can be expressed as

$$a = 2c = 0, \quad t = 0. \tag{1}$$

From the crack depth and length data shown in Figure 2, the following relation can be established to describe the relationship between a and c:

$$a = m \cdot \ln(n \cdot c + 1), \tag{2}$$

wherein m and n are the fitting parameters which could be obtained by fitting the field crack depth and length data using Eq. [2]. One could deduce from Eq. [2] that a is zero when c is zero.

B. *Boundary Condition 2*

Since the environmental conditions along the crack length and in the depth direction at beginning of crack initiation are the same, boundary condition II can be defined as

$$\frac{\mathrm{d}a}{\mathrm{d}t} = \frac{\mathrm{d}c}{\mathrm{d}t}, \quad t = 0. \tag{3}$$

Differentiating Eq. [3] yields

$$\frac{\mathrm{d}a}{\mathrm{d}t} = \frac{\mathrm{d}a}{\mathrm{d}c} \cdot \frac{\mathrm{d}c}{\mathrm{d}t} = \frac{m \cdot n}{n \cdot c + 1} \cdot \frac{\mathrm{d}c}{\mathrm{d}t}. \tag{4}$$

Since c is 0 at $t = 0$, Eq. [4] could be simplified as

$$\frac{\mathrm{d}a}{\mathrm{d}t} = m \cdot n \cdot \frac{\mathrm{d}c}{\mathrm{d}t}, \; t = 0. \tag{5}$$

From Eq. [3], the relationship between parameters m and n can be found as

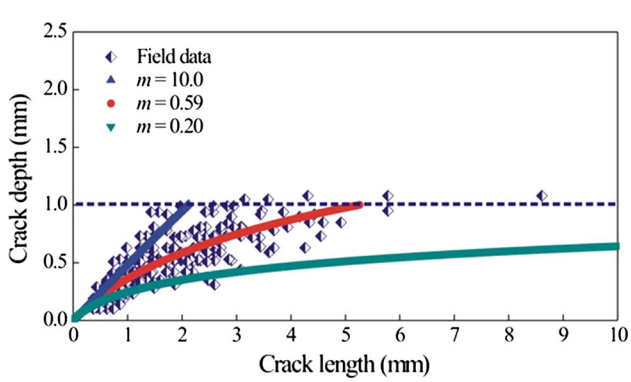

Fig. 4—Comparison between the field data and fitting curve on relation of crack depth and length in the stage I (when crack depth is less than 1.0 mm).

$$m \cdot n = 1. \tag{6}$$

Therefore, Eq. [2] could be simplified as

$$a = m \cdot \ln\left(\frac{c}{m} + 1\right). \tag{7}$$

As a result, crack depth, a, and crack length, $2c$, could be related through Eq. [7] using a single parameter m. Eq. [7] is used to curve fit the field data shown in Figure 4. The red curve in Figure 4 with $m = 0.59$ was generated by best fitting all the data available, while the other two fitting curves with m equal to 10.0 and 0.20 represent the upper boundary and lower boundary of crack depth–length relationship, respectively.

C. *Boundary Condition 3*

It has been widely observed that NNpH cracks reach a dormant state at a crack depth of about 1.0 mm deep.[24] This occurs because crack growth through direct dissolution of material at the crack tip becomes very low, although it is not equal to zero (completely dormant) according to recent experimental findings which will be further discussed. From this, boundary condition 3 is defined as

$$\frac{\mathrm{d}a}{\mathrm{d}t} = h, \quad a = 1.0 \text{ mm}, \tag{8}$$

where h represents the stable value of crack growth rate in the depth solely caused by dissolution of the crack tip material, which could be measured and determined experimentally (see Section V for details).[11] Therefore, according to Eq. [4], we could have

$$\begin{cases} \dfrac{\mathrm{d}a}{\mathrm{d}t} = e^{-\frac{a}{m}} \cdot r, & a \leq 1.0 \text{ mm} \\ r = \dfrac{\mathrm{d}c}{\mathrm{d}t}, & t = 0 \text{ and } a = 0 \end{cases}, \tag{9}$$

where r is the crack growth rate by dissolution along the pipe surface, which could be regarded as a constant during crack propagation because the surface is assumed to be fully exposed to the same near-neutral environment during the process of cracking. Hence, the general expressions of $\frac{\mathrm{d}a}{\mathrm{d}t}$ could be written as follows:

$$\frac{\mathrm{d}a}{\mathrm{d}t} = \begin{cases} e^{-\frac{a}{m}} \cdot r, & a \leq 1.0 \text{ mm} \\ h, & a > 1.0 \text{ mm} \end{cases}. \tag{10}$$

V. DETERMINATION OF CONSTANTS OF THE GOVERNING EQUATIONS FOR CRACK INITIATION AND EARLY-STAGE GROWTH

Equations [7] through [9] can be used to predict early-stage crack growth if the three constants r, h, and

m, can be determined accurately. They are discussed below:

- Determination of r
  r can be considered to be a constant for a given crack because of the essentially constant environmental conditions on the pipeline surface when the crack dimension is small and when mechanical driving forces play little role in crack growth. One can assign r a value that is equal to the crack growth rate corresponding to the rate of dissolution determined by exposing a bare pipeline steel to NNpH environments. For example, the crack growth rate determined based on the rate of dissolutions of a bare X-65 was in the range of 0.6×10^{-9} to 1.2×10^{-9} mm/s, as listed in Table I for various NNpH solutions.[10] Taking a crack growth rate of 9×10^{-10} mm/s and using $m = 0.59$, it would take about 93.5 year for the crack to reach a depth of 1.0 mm.
  Assigning r a rate corresponding to the dissolution rate of bare steel is obviously not consistent with reality. The initial rate of crack growth through dissolution should be much higher than the rate corresponding to the dissolution rate of bare pipeline steel. It has been determined that galvanic corrosion either between cracked mill scale and the bare steel at the bottom of the mill scale cracks,[23] or between regions with different residual stresses[13] is responsible for the initial enhanced crack initiation and growth. Since the actual rate of corrosion under such a galvanic condition is hard to determine, the value of r could not be determined directly, but could be obtained indirectly if the value of h can be determined, which is discussed next.
- Determination of h value:
  h is the crack growth rate caused by the direct dissolution of crack tip material. This rate should be very low, lower than the crack growth rate calculated based on the dissolution rate of bare steel exposed to NNpH environments. h is the lowest crack growth rate caused by direct dissolution and therefore could also be considered to be the crack growth rate attributed to the direct dissolution of the crack tip material in Stage II. The very minor contribution of dissolution to crack growth has been confirmed experimentally in several investigations reported previously.[28–30]
  Because passivation of the steel surface does not occur in NNpH environments h can be measured directly from experiments, which could be considered to be equal to the net half width of the crack crevice after corrosion fatigue testing under loading conditions in Stage II. This net half width of a crack is defined as the half width of crack crevice after corrosion fatigue minus the half width of crack crevice after testing in air under the same mechanical loading using CT specimens with the same initial geometry. The width of crack crevice was usually measured at 5 μm from the crack tip after pre-fatigue cracking in air on the middle section of a CT specimen after corrosion fatigue.[11]
  Table II lists the net half width of crack crevice from a number of tests of a X-65 pipeline steel in C2 solution. To obtain a h value with statistical significance, h is defined as

$$h = \sum_{j=1}^{k} \frac{\mathrm{d}a}{\mathrm{d}t}(k) \cdot p(k) \quad \text{for} \quad a \geq 1.0\,\text{mm}, \qquad [11]$$

  where h is the crack depth growth rate caused solely by the dissolution of the crack tip material when crack depth reaches 1.0 mm and beyond; k is the total number of tests; $\frac{\mathrm{d}a}{\mathrm{d}t}(k)$ is the average crack growth rate by dissolution of k tests and the $p(k)$ is the probability percentage of the kth test in Table II which has listed 11 h-values obtained from experiments. Table II displays the distribution of h values. From Eq. [11], h is determined to be 7.69×10^{-10} mm/s.
  The crack growth rate corresponding to the dissolution rate of a bare X-65 pipeline exposed to C2 solution was determined to be 1.41×10^{-9} mm/s[26] which is higher than the value of h determined for the reasons indicated previously. A crack is considered to be dormant when it grows at a rate of h, that is, crack growth at such a rate would be too slow to be a concern and failure of pipeline steels would occur well after the design limit of service life (even considering that the design limit of service life may not be well defined). For example, it takes over

Table I. Stable Surface Dissolution Growth Rate for Four Kinds of Near-Neutral Solutions[10]

Solution Items	NOVATW	NS4	C1	C2
Dissolution rate	6.00×10^{-10} mm/s	9.00×10^{-10} mm/s	1.2×10^{-9} mm/s	1.14×10^{-9} mm/s

Table II. Details of Experimental Results on Dissolution Rate on Depth Direction When Crack Depth Is Larger than 1.0 mm

Items	1	2	3	4	5	6	7	8	9	10	11
Test time (days)	65	48	50	45	39	38	38	54	41	30	30
Average dissolution rate (unit: 10^{-10} mm/s)	5.48	7.68	7.27	9.93	8.70	7.55	7.68	6.51	6.09	8.94	8.82

The dissolution rate was calculated by using the net half width of crack crevice before and after tests.

100 years for a crack to advance to about 40 pct wall thickness by crack tip dissolution at a rate of 7.69×10^{-10} mm/s. It should be pointed out that the possibility of failures solely induced by the failure pressure was not considered here since the emphasis of this work is the fatigue crack growth model.

From Eq. [10], r is calculated to be 4.19×10^{-9} mm/s at $h = 7.69 \times 10^{-10}$ mm/s and $m = 0.59$. This r value is significantly higher than the crack growth rate determined based on the dissolution rate of a bare X-65 pipeline steel exposed to C2 solution. This reflects the enhanced corrosion caused by galvanic effects at or in the vicinity of steel surface.[23] A crack would reach 40 pct wall thickness in 27 years if the crack growth rate (4.19×10^{-9} mm/s) corresponding to the high dissolution rate at the pipeline surface is maintained. This is obviously not realistic since the high dissolution rate at pipeline surface decreases rapidly as the crack propagates. The growth curve at $r = 4.19 \times 10^{-9}$ mm/s and $h = 7.69 \times 10^{-10}$ mm/s in Figure 5 represents an average scenario of crack growth by dissolution, under which the lifetime spent in Stage I (up to 1.0 mm) is about 20 years. This Stage I lifetime is still too long to cause a premature failure of pipeline steels in 20 to 30 years as normally found in the field. This discrepancy reflects the fact that the failure was always caused by one crack with the fastest crack growth rate which can be possible only when all the worst conditions for crack initiation and growth are met. The best fitted line does not represent the worst conditions. The latter situation is to be further discussed.

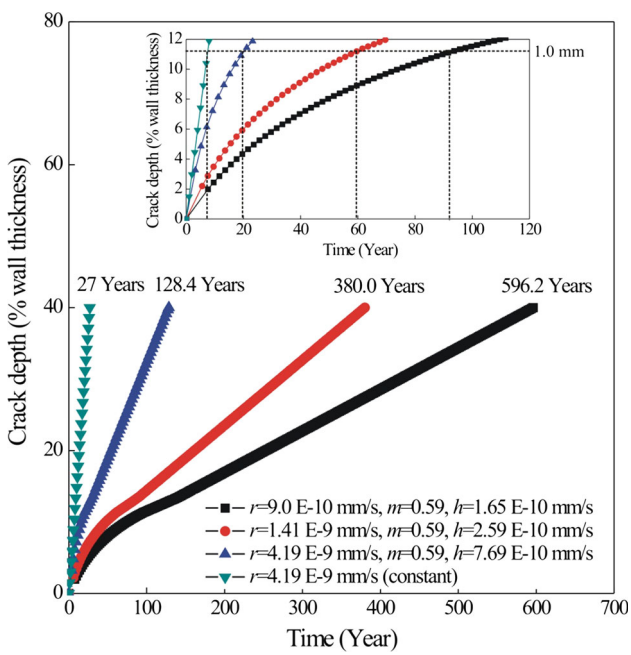

Fig. 5—Comparison of life prediction based on model basics. Here, only dissolution was considered. Wall thickness of the pipe is 8.9 mm.

- Determination of m value:

  Parameter m is obtained by fitting the data from the field, which yields a high degree of statistical significance and relevance to the cracking in the field. It may vary with a number of factors including different soil environments[10] and with the strength, composition, and microstructure of the pipeline steels. The upper and lower limits of the crack depth–length curves are also shown in Figure 4, which were obtained by curve fitting the data by assigning Eq. [7] with different m values. Different values of m could be related to the different dissolution rates of soil environments, galvanic behavior, and materials resistance to dissolution. In particular, a crack depth–length profile with high m value would correspond to a crack shape approaching to a semi-circle, which is not typical of NNpH cracks. A crack depth–length profile with low m value is associated with cracks having large crack length/depth ratios and is very typical of NNpH stress cracks. Further discussion will be made later to elucidate the selection of m value

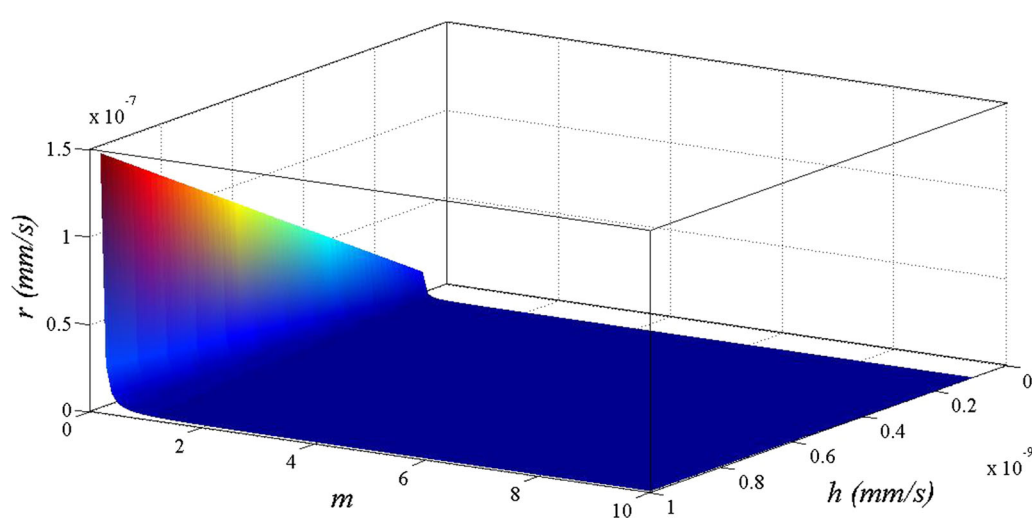

Fig. 6—Correlation of r with different settings of value of r, m, and h.

representing the worst scenario of crack initiation and early-stage crack growth.

The above discussion on the determination of various constants in Eq. [10] demonstrates that Eq. [10] is a general governing equation suitable for a wide range of corrosion conditions in NNpH environments. This is further illustrated in Figure 6 in which a wide range of crack growth profiles could be obtained by adjusting the three constants discussed above.

VI. PREDICTION OF CRACK GROWTH IN STAGE I

One of the key features of NNpH SCC is that over 95 pct of cracks found in crack colonies remained dormant and only less than 5 pct of them were able to grow out of the dormant state.[24] It is therefore important to determine the conditions at which a crack would either remain dormant or become active.

In order for a dormant crack to become active, the crack growth rate in Stage II must be in the high end of the range. Details of Stage II modeling and mechanisms are to be presented in Reference 27. To make a simple demonstration, a gas pressure spectrum with moderate pressure fluctuations in terms of crack growth rate in Stage II was used to generate a crack growth curve which is superimposed onto various crack growth curves in Stage I. As shown in Figure 7, it takes about 52.6 years for a crack to grow to 40 pct wall thickness when Stage II growth is superimposed, a significant reduction of service life as compared with the prediction made by dissolution model alone.

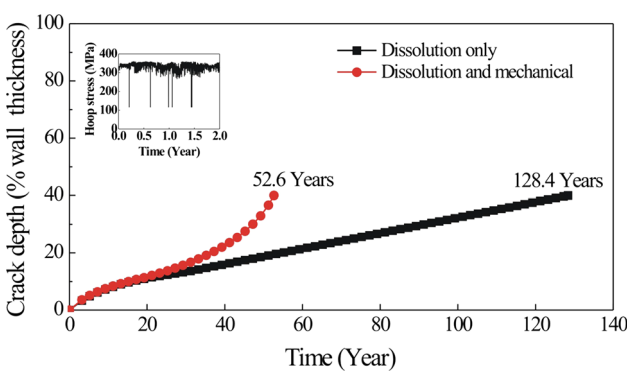

Fig. 7—Life prediction with or without considering mechanical contribution. Wall thickness of the pipe is 8.9 mm.

To demonstrate a wide range of situations where a crack could remain dormant or become active, the upper curve, the best fit, and the lower dissolution growth curves based on the upper, the best fit, and lower crack depth–length ($a \sim 2c$) profiles shown in Figure 4 were also modeled with an incorporation of Stage II growth. For the purpose of comparison, the $a \sim 2c$ profiles in Figure 4 were mathematically fit to generate crack growth rate functions using the same r value. As shown in Figure 8, a wide range of predicted lives is seen. In Figure 8(b), the best fit $a \sim 2c$ profile shown in Figure 4 has yielded a predicted life of 52.6 year, about 2.4 times shorter than the life predicted solely based on the dissolution model (in Figure 7) reflecting the contribution of crack growth in Stage II.

On the other hand, the upper bound $a \sim 2c$ curve in Figure 4 yields a life of 22.2 years, which is only 5 years shorter than the life predicted based on the dissolution model shown in Figure 5. Such a prediction is inconsistent with the general observation that crack growth by dissolution in Stage II is minimal and therefore the prediction must be regarded as tenuous.

As illustrated in Figure 8(a), the upper bound $a \sim 2c$ profile in Figure 4 has yielded a $da/dt \sim a$ curve with very benign changes in da/dt with a. This disagrees with the observation of crack dormancy caused by much reduced crack growth rate as crack grows. It is also contrary to the fact that NNpH cracks have large length/depth ratios, usually in the range of 5 to 20. The upper bound curve in Figure 8(a) would yield an aspect ratio close to 2 (semi-circular shape), which is the observed crack growth profile of high-pH stress corrosion cracks. Therefore, the top curve in Figure 8(a) representing the upper bound a–c relation in Figure 4 must be regarded as unrealistic.

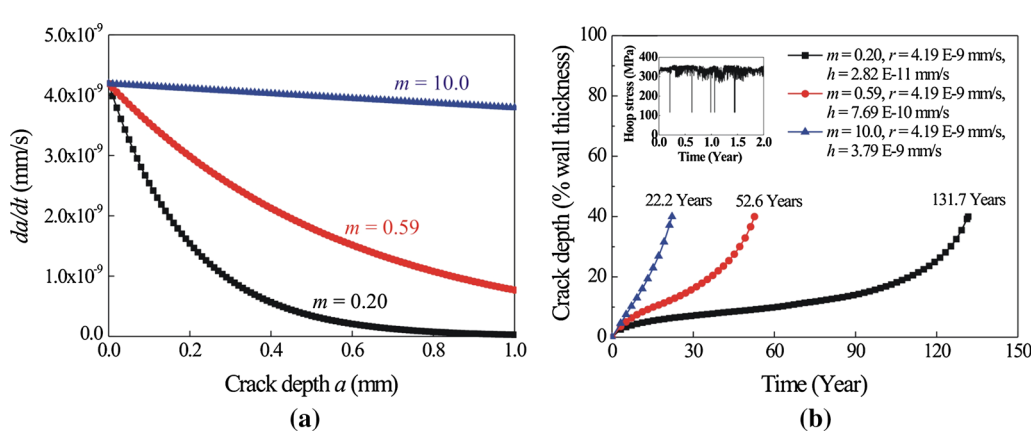

Fig. 8—Effects of dissolution conditions on the transition of dormant state. (*a*) Dissolution growth rate in depth $\frac{da}{dt}$ with crack depth evolution a for three typical solution conditions; (*b*) comparison on the transition of dormant state and predicted life.

For the upper bound curve shown in Figure 8(a), the value of m is fixed as it was obtained by curve fitting the upper bound a–c data in Figure 4. This leaves r or h as the only variable to be adjusted in order to generate a reasonable growth curve such as shown in Figure 8(b). The $da/dt \sim a$ curves in Figure 8(a) were generated by using the same r value. This is obviously incorrect. For the upper bound a–c curve with high m value, a low r value would be more reasonable since the life is longer corresponding to less corrosion, while the lower bound a–c curve with a low m value should have a high r value since the life is shorter corresponding to more corrosion. This is illustrated in Figure 9(a), and it is assumed that h is constant. It is believed that the $da/dt \sim a$ profiles in Figure 9(a) are reasonable and closer to reality. Some justifications are given below:

(a) An a–c curve with a high m value representing a situation with minimum difference in crack growth rate between the deep tip and surface tip. This could be achieved by either of the following two scenarios:

  i. A higher dissolution rate in the depth direction at certain locations of pipeline steels. For example, this could be caused by varied metallurgical conditions in the pipeline steel. This is unlikely considering the metallurgical variables are usually at micrometer scale while dissolution dominant processes exist over a range up to 1.0 mm.

  ii. A reduced dissolution rate at surface. For example, (1) at regions with partial cathodic protection where fast corrosion is prohibited, (2) because of the limited length of cracks in mill scale, which restricts further dissolution on the pipe surface, and (3) when crack initiation occurs in regions with lower CO_2 level because of lower CO_2 content in soil environments or the cracking position further from the open mouth of a disbonded holiday.

(b) An a–c curve with low m value representing a situation with a large difference in crack growth rate between the depth tip and the surface tip. The same justification as in (a) could be applied here:

  i. A lower dissolution rate in the depth direction within certain locations of pipeline steels, which is unlikely the case as indicated in (a)-i.

  ii. An increased dissolution rate at surface. This is quite likely under such circumstances as, (1) in regions without effective cathodic protection where fast corrosion is not prohibited, (2) because of the long length of cracks in mill scale which does not restrict further dissolution on pipe surface, and (3) when crack initiation occurs in regions with higher CO_2 level because of higher CO_2 content in soil environments or with crack initiation sites closer to the open mouth of a disbonded holiday.

The illustration in Figure 9 suggests a very minor variation of h value (assumed to the same in this case), which can be justified because of the crack dormancy commonly occurring in NNpH environments. From Figure 9, it is inferred that a da/dt–a curve with high m value (10) would yield the longest Stage I growth, while the $da/dt \sim a$ curve with low m value (0.2) representing lower bound a–$2c$ relation have the shortest Stage I growth.

The lower bound a–$2c$ profile in Figure 4 produces a crack growth rate at the surface as high as 1.14×10^{-7} mm/s. Such a high growth rate has been found during the simulation of the enhanced crack initiation and growth caused by the galvanic process established between regions with different levels of residual stresses.[13] In the latter case, a crack with a depth of 0.74 mm was initiated after stress corrosion exposure in C2 solution under a benign cyclic loading scheme for 2631 hours. This yields an average crack

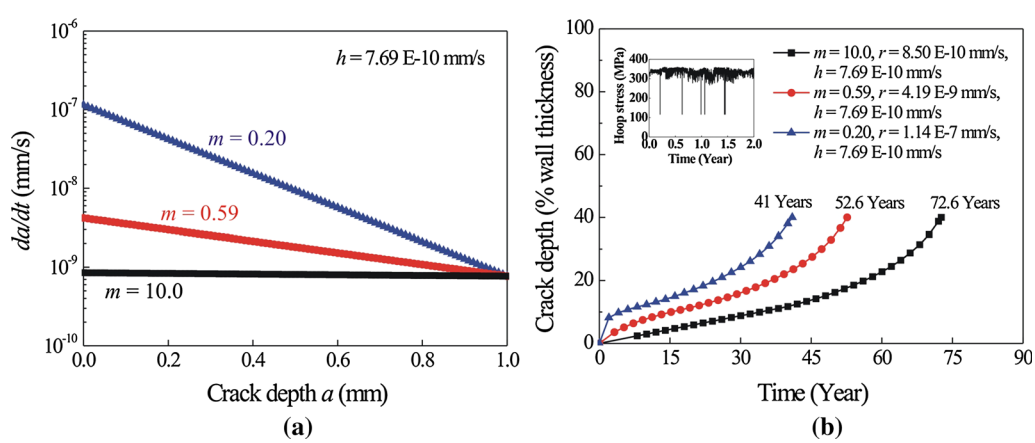

Fig. 9—Life prediction by assuming same h value but different m values: (a) different crack growth rate–depth profiles, (b) predicted lives corresponding to different crack growth rate–depth profiles in (a).

growth rate as high as 0.78×10^{-7} mm/s. Assuming an *a–2c* curve with $m = 0.2$, the value of r is estimated to be 8.33×10^{-7} mm/s $\left(\text{obtained by solving } \int_0^{0.74} e^{\frac{a}{m}} \cdot \mathrm{d}a = \int_0^{2631\mathrm{h}} r \cdot \mathrm{d}t\right)$. This is even higher than the crack growth rate of 1.14×10^{-7} mm/s (the blue curve in Figure 9), which was determined based on the lower bound *a–2c* curve shown in Figure 4. When $r = 8.33 \times 10^{-7}$ mm/s is used for life prediction and assuming $m = 0.2$, the service life of the pipeline steel with the same pressure fluctuation shown in Figure 9 is estimated to be 11.6 years. With the consideration of incubation time required before crack initiation, which is usually about 12 years on average, the total service life from the time of installation to the time of failure would be about 23.6 years, in agreement with the actual pipeline life commonly found in the field.

VII. TRANSITION FROM DORMANT STATE TO ACTIVE GROWTH

Besides the effect of dissolution behavior on Stage I crack growth, the other factor that could play a role in extending or shortening the period of dormancy is the residual stresses present in pipeline steels. Depending on the nature and magnitude of compressive or tensile stresses, the residual stresses could be added to the externally applied stresses to increase or decrease the mechanical driving forces the onset of crack growth in Stage II.

Among all the efforts made on the effect of residual stresses, a noteworthy study by Beavers *et al.*[3] on steel line pipe using a hole drilling technique has shown that the mean residual stress near the SCC colonies was about twice as high as in the control areas and the difference was highly statistically significant at a 99.98 pct confidence level. The average residual stress for the SCC colonies was 216 MPa with a standard deviation of 104 MPa. This gives a lower bound tensile residual stress for SCC colonies of 112 MPa.

For plastically deformable materials, the residual and applied stresses can be added together directly until the yield strength is reached.[31] For a X-65 pipeline steel operated at 75 pct SMYS (Specified Minimum Yield Strength), the maximum additional tensile residual stresses that can be added would be about 110 MPa ($= 0.25 \times 455$ MPa $= 113$ MPa). This value is surprisingly consistent with the minimum residual stresses found in SCC colonies, as indicated previously.

Under a plastically deformed state without applying external stresses the highest residual stresses can be as high as 300 MPa (tensile) and as low as −300 MPa (compressive).[13,14] Because the net residual stresses in a given free body must integrate to zero over any cross-sectional area, regions with high tensile residual stresses must be balanced by regions with compressive stresses. Based on these principles, and with a reference to some typical distributions of residual stresses measured in deformed pipeline steels,[13,14] five patterns of residual stresses that could be added to the applied tensile stresses generated by internal pressures have been constructed. These are shown in Figure 10, in which the initial maximum and minimum residual stresses were assumed to be ±300 MPa, respectively. Although the total tensile stress in regions with compressive stresses is well below the yield tensile strength (it is approximated by the SMYS in this case), the actual compressive residual stresses were also adjusted to achieve zero net force for a given residual stress profile.

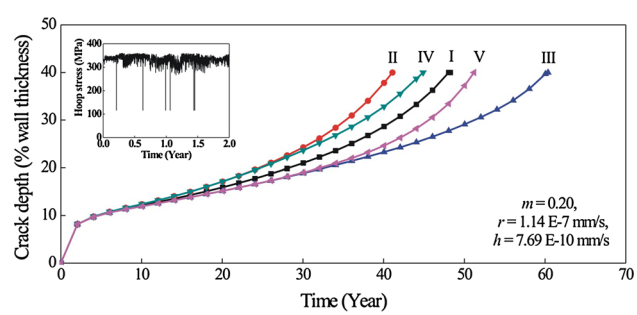

Fig. 11—Residual stress effects on life prediction when m is 0.20.

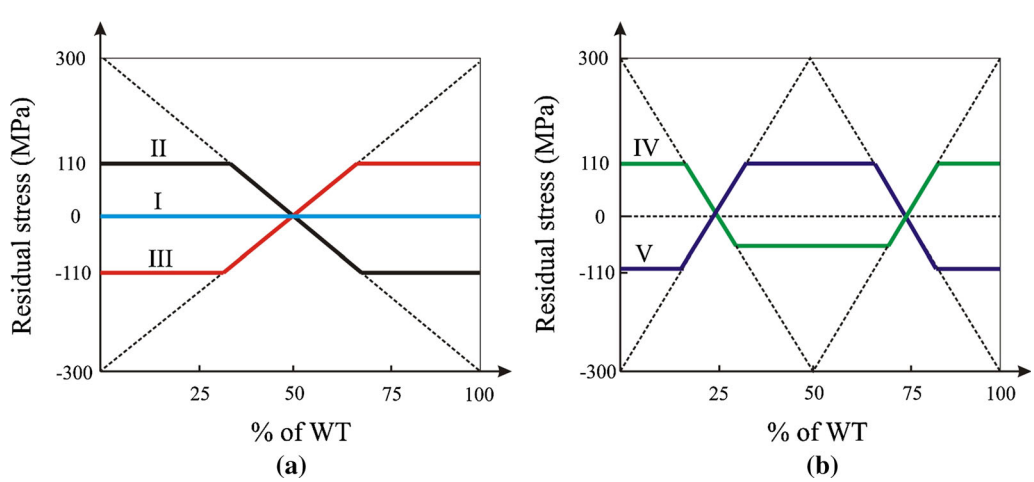

Fig. 10—Five tracks of residual stress *vs* percent of wall thickness (WT): (*a*) track I to III, (*b*) track IV and V.

The predicted crack service life, up to 40 pct wall thickness, is shown in Figure 11. It is clear that the effect of residual stresses is significant. Residual stress profile III with compressive stresses present near the pipe surface where cracks are initiated has shown the longest predicted life while profile II yields the shortest service life. The presence of compressive stresses within 1.0 mm of the pipe surface has caused a minor extension of service life because of the predominant dissolution-controlled growth.

The above discussion has provided a wide range of situations in which a dormant crack could either remain dormant or become active. It appears that the premature rupture by NNpH SCC at a service life of about 20 to 30 years commonly found during field operation could take place only when the worst scenarios have been concurrently realized at the site of rupture. The worst scenarios in terms of pipeline lifetime spent in crack initiation and early-stage crack growth may include:

1. The earliest occurrence of coating damage and access of ground water to the surface of pipeline steel enabling the occurrence of corrosion.
2. A disbonded coating geometry and aqueous chemistry that prevents the reach of cathodic current to the surface under the disbondment.
3. A high level of tensile residual stresses at the pipe surface where galvanic corrosion could take place, which may lead to the formation of pits and cracks at the bottom of pits.
4. A ground water chemistry that is most susceptible to cracking, which was found to be the one with a pH around 6.5, according the field data and experimental simulations.[10,32]
5. A high level of tensile residual stresses maintained over a distance to the pipeline surface at which a crack has become dormant, which would shorten the time to the onset of Stage II crack growth.
6. A pipeline section where frequent pressure fluctuations of large amplitudes, such as hydrostatic tests, are encountered, which could sharpen a dormant crack usually having blunt tip for active growth.

Scenario (1) in the above list is related to the preparation process for the onset of corrosion, Scenarios (2) to (4) are directly related to the process of crack initiation and early stage of crack growth, and Scenarios (5) and (6) determine the length of time a crack could remain dormant. The crack data from the field shown in Figure 4 only reflect Scenarios (2) to (4), which involves a direct interaction of environments with susceptible steels. The worst scenarios corresponding to the shortest time spent in Stage I behavior and final rupture is also largely dependent of Scenario (1), (5), and (6). The latter scenarios can be inter-related because the site with the earliest occurrence of corrosion [Scenario (1)] will also have experienced the longest history of critical pressure fluctuations [Scenarios (5) and (6)] that could re-activate a dormant crack. Considering the fact that a material's heterogeneity exists over a relatively small-scale range (μm for microstructural heterogeneity and that processing and fabrication heterogeneity exists over a scale of millimeter to meters and that environmental conditions can be considered relatively consistent within a few meters around the rupture site, the process of crack initiation and early crack growth [Scenarios (2) to (4)] for those cracks shown in Figure 4 could be comparable to the process in the crack colony where the rupture had occurred. Therefore, the crack data shown in Figure 4 can be considered to be typical and entail a whole range of Stage I behavior including the worst one.

The above discussion of the worst scenarios also explains why over 95 pct of NNpH cracks remain harmless, while about 1 pct of them become a threat to the integrity of pipeline steels. Please note that this paper has not considered the wide range of operating conditions affecting the Stage II crack growth,[27] which could also play an important role in dormant–active transition.

It should be noted that the current modeling of crack initiation and the occurrence of crack dormancy could be further improved in a number areas, which include but are not limited to:

- Pressure fluctuation-dependent dissolution behavior, especially at depth tip of a crack: as to be introduced in Reference 27, pressure fluctuates very differently during operation of gas pipelines and oil pipelines. Different types of pressure fluctuations may lead to a varied diffusion kinetics of ions involved in the electrochemical process of corrosion and therefore different rates of corrosion.
- Crack geometry-dependent dissolution and dormancy behavior: NNpH SCC cracks normally have a large $2c/a$ (crack surface length/crack depth) ratio in Stage I. Increasing $2c$ but maintaining crack depth a will lead to a reduction of stress intensity factor, K, at the crack surface tip but an increase of K at the depth tip. Under the circumstances, revision of the current model is needed to reflect the following changes: (1) reduced rate of corrosion at the surface tip and/or increased rate of corrosion at the depth tip possibly because of stress/plasticity-assisted dissolution at the crack tip, (2) possible formation of a galvanic couple between the surface tip and the depth tip with much enhanced dissolution rate at the depth tip and the suppression of dissolution at the surface tip, (3) possible onset of Stage II crack growth at the depth tip of the cracks with large $2c/a$ ratios despite that crack depth is relatively small.
- Effect of cathodic potential on crack growth: Although crack initiation is believed to occur at the pipe steel surface without or with insufficient cathodic protection, cathodic protection could be reached later to the steel surface with SCC colonies. Preliminary investigation has found different crack growth behaviors at the surface tip and at the depth tip. The model for stage I could be revised to reflect the worst scenario related to cathodic protection.

From the viewpoint of pipeline integrity management, modeling of crack initiation and early-stage crack growth in Stage I is less engineering significant than modeling of Stage II crack growth behavior. This is because crack dimension in Stage I is small, usually at around or less than 1.0 mm, which is not detectable during in-line inspections, and would not cause premature failure of pipeline steels if Stage II mechanisms will not be operative. However, both stage I and stage II together define the worst scenario responsible for pipeline failures. The initial detection of cracks by in-line inspections provides an opportunity of calibrating the stage I model, from which key modeling parameters used in modeling both for stage I and stage II can be traced. It is also believed that methodology adopted in stage I modeling could be applied to other structure systems with SCC failures in terms of designing and/or processing the materials, and developing operational strategies avoiding the risk of SCC failures.

VIII. CONCLUSIONS

This paper has focused on the modeling of crack initiation and early-stage crack growth of pipeline steels in NNpH environments.

1. Mathematical equations governing crack initiation and early-stage crack growth have been developed based on the characteristics of the cracks examined in the field and the current understanding of crack initiation and growth mechanisms in NNpH environments.
2. The investigation has modeled a wide range of conditions that could lead to crack initiation, crack dormancy, and the transition from a dormant state to active growth.
3. It is concluded that the premature rupture by NNpH SCC at a service life of about 20 to 30 years commonly found during field operation could take place only when the worst conditions responsible for crack initiation and growth have been realized concurrently at the site of rupture. This also explain the reason why over 95 pct of NNpH cracks remain harmless, while about 1 pct of them become a threat to the integrity of pipeline steels.

ACKNOWLEDGMENTS

The authors would like to thank TransCanada Pipeline Limited, Spectra Energy Transmission, Natural Science and Engineering Research Council of Canada, the Pipeline Research Council International (PRCI) and US Department of Transportation for financial support.

REFERENCES

1. National Energy Board: *Public Inquiry Concerning Stress Corrosion Cracking on Canadian Oil and Gas Pipelines*, National Energy board, November, 1996.
2. J.A. Beavers: Report prepared for the Gas Research Institute, GRI-7045, 2004.
3. J.A. Beavers, J.T. Johnson, and R.L. Sutherby: *Proceedings of 3th International Pipeline Conference*, vol. 2, Calgary, Canada, October 1–5, 2000, pp. 979–88.
4. CEPA: *Stress Corrosion Cracking Recommended Practices*, 2nd edn, CEPA, Calgary, 2007.
5. PL Andresen and FP Ford: *Mater. Sci. Eng. A.*, 1988, vol. 103, pp. 167–84.
6. PL Andresen and FP Ford: *Int. J. Pres. Ves. Pip.*, 1994, vol. 59, pp. 61–70.
7. F.P. Ford, D.F. Taylor, P.L. Andresen, and R.G. Ballinger: EPRI Final Rep. NP-5064M, Electric Power Research Institute, 1987.
8. W. Zheng, W. Revie, F.A. MacLeod, and O. Dinardo: Pipeline Research Council International (PRCI), Houston, USA, 2000, Category No. L51791E.
9. J. Been and R.L. Sutherby: *NACE Northern Area Western Conference*, Calgary, Canada, February 7–8, 2006.
10. WX Chen and RL Sutherby: *Metall. Mater. Trans. A*, 2007, vol. 38A, pp. 1260–68.
11. M.S. Yu: PhD thesis, University of Alberta, 2015.
12. WX Chen, F King, and ED Vokes: *Corrosion*, 2002, vol. 58, pp. 267–75.
13. G Van Boven, WX Chen, and R Rogge: *Acta Mater.*, 2007, vol. 55, pp. 29–42.
14. WX Chen, G Van Boven, and R Rogge: *Acta Mater.*, 2007, vol. 55, pp. 43–53.
15. D. He, T.R. Jach, F. King, and W.X. Chen: *International Pipeline Conference*, 2000, vol. 2, 2002, p. 997.
16. M. Elboujdaini, Y.Z. Wang, R.W. Revie, R.N. Parkins, and M.T. Shehata: *Proceedings of Corrosion 2000*. NACE, Houston, TX, 2000, Paper No. 00379.
17. WX Chen, SH Wang, R Chu, F King, TR Jack, and RR Fessler: *Metall. Mater. Trans. A*, 2003, vol. 34A, pp. 2601–08.
18. R Chu, WX Chen, SH Wang, F King, TR Jack, and RR Fessler: *Corrosion*, 2004, vol. 60, pp. 275–83.
19. T. Kushida, K. Nose, H. Asahi, M. Kimura, Y. Yamane, S. Endo, and H. Kawano: *Proceedings of Corrosion 2001*. NACE, Houston, TX, 2001, Paper No. 01223.
20. SH Wang, WX Chen, F King, TR Jack, and RR Fessier: *Corrosion*, 2002, vol. 58, pp. 526–34.
21. BY Fang, RL Eadie, WX Chen, and M Elboujdaini: *Corros. Eng. Sci. Technol.*, 2009, vol. 44, pp. 32–42.
22. BY Fang, RL Eadie, WX Chen, and M Elboujdaini: *Corros. Eng. Sci. Technol.*, 2010, vol. 45, pp. 302–12.
23. Z Qin, B Demko, J Noel, D Shoesmith, F King, R Worthingham, and K Keith: *Corrosion*, 2004, vol. 60, pp. 906–14.
24. WX Chen, R Kania, R Worthingham, and G Van Boven: *Acta Mater.*, 2009, vol. 59, pp. 6200–14.
25. A Egbewande, WX Chen, R Eadie, R Kania, G Van Boven, R Worthingham, and J Been: *Corros. Sci.*, 2014, vol. 83, pp. 343–54.
26. K. Chevil: Master Thesis, University of Alberta.
27. J.X. Zhao, W.X. Chen, M.S. Yu, K. Chevil, R. Eadie, J. Been, G. Van Boven, R. Kania, and S. Keane: *Metall. Mater. Trans. A.* unpublished data.
28. MS Yu, WX Chen, R Kania, G Van Boven, and J Been: *Fatigue Fract. Eng. Mater. Struct.*, 2015, vol. 38, pp. 681–92.
29. MS Yu, X Xing, H Zhang, JX Zhao, R Eadie, WX Chen, J Been, G Van Boven, and R Kania: *Acta Mater.*, 2015, vol. 96, pp. 159–69.
30. YW Kang, WX Chen, R Kania, G Van Boven, and R Worthingham: *Corros. Sci.*, 2011, vol. 53, pp. 968–75.
31. P.J. Bouchard: *Encyclopedia of Materials Science and Technology, IV: Structural Phenomena*, K.H.J. Buschow et al., eds., Elsevier, Oxford, Pergamon, 2001, pp. 8134–42.
32. EB Delanty and J O'Beirne: *Oil Gas J.*, 1992, vol. 90, pp. 39–45.